RSC Advances

ROYAL SOCIETY OF CHEMISTRY

www.rsc.org/advances

Inhibition of copper corrosion in cooling seawater under flowing conditions by novel pyrophosphate

M. A. Deyab[1*], R. Essehli[2], B. El Bali[3]

[*1]Egyptian Petroleum Research Institute (EPRI), Nasr City, Cairo, Egypt

*Corresponding author. Tel.: +201006137150; fax: + 202 22747433

*E-mail addresses: hamadadeiab@yahoo.com

[2]Qatar Environment and Energy Research Institute (QEERI), PO Box 5825, Doha, Qatar, E-mail: ressehli@qf.org.qa

[3]Laboratory of Mineral Solid and Analytical Chemistry "LMSAC", Department of Chemistry, Faculty of Sciences, University Mohamed I, PO. Box 624, 60000 Oujda, Morocco

Abstract

Inhibition of copper corrosion in cooling seawater by novel pyrophosphate molecule $SrNiP_2O_7$ (SNP) was investigated under flowing conditions by using mass loss and electrochemical methods. The surface morphology was characterized by SEM coupled with EDX spectra. Comparable results show that SNP acts as a mixed-type inhibitor with predominantly cathodic effectiveness, suppressing corrosion process by physical adsorption on copper surface. The highest inhibition efficiency obtained from mass loss, polarization and EIS measurements are 92.7, 94.8 and 97.1% respectively at 120 mg/L of SNP. The influence of the temperature rising on the inhibitor efficiency of SNP has been studied and activation energy has been

calculated. Surface morphology observations evidenced the formation of a protective film of SNP over metal surface.

Keywords: inorganic compounds; copper; corrosion test; electrochemical techniques; seawater

1. Introduction

Cooling water systems are widely used in oil refineries and in chemical plants, as well as in homes, factories and public buildings [1]. These may be classified generally into two types [2]. First type is the once-through cooling system, and the second type is the recirculating cooling water system. Corrosion problems in the second system are generally very high. Seawater is a commonly used fluid in cooling systems, particularly coastal zone [3].

Copper is a material widely used in cooling systems for domestic and industrial water utilities, including seawater, heat conductors, and heat exchangers [4]. In spite of the relatively corrosion resistance of copper, its corrosion takes place at a significant rate in seawater [5-7].

The use of inorganic inhibitors is one of the most practical and effective methods for protection of the copper in cooling systems [8-9]. Generally, chromate is accepted as a famous corrosion inhibitor, where it can passivate metals by forming a mono-atomic or poly-atomic oxide film at the metal surface. However, the main disadvantage of using chromate is chromate toxicity [10].

Environmental regulations drive researchers to increase their efforts to develop and evaluate new nontoxic inorganic inhibitors to replace traditional inorganic inhibitors

such as chromate. In view of these environmental regulations, the SNP was synthesized for the present work.

Recently, pyrophosphates are of considerable industrial and biological importance because of their utility in various applications as catalysts, molecular sieves, or ion exchangers [11].

Generally, different types of pyrophosphates such as tetrasodium pyrophosphate and phosphate glass have been used as corrosion inhibitors in different aggressive solutions [12-16]. These inhibitors were found to act successfully as corrosion inhibitors of steel and copper. The corrosion inhibition efficiencies of these inhibitors are in range 80–95%.

The novelty in this study concerns the influence of novel pyrophosphate molecule $SrNiP_2O_7$ (SNP) on the corrosion inhibition of copper in recirculating cooling seawater. Novel pyrophosphate molecule $SrNiP_2O_7$ could be consider as an effective potential inhibitor owing to containing electronegative O-heteroatom, In addition, it is non-toxic. While to our limited knowledge, no reports or research works, regarding the use of $SrNiP_2O_7$ as potent corrosion inhibitor.

The inhibiting performance has been evaluated by mass loss, polarization and electrochemical impedance spectroscopy (EIS) measurements. The surface morphology of copper was examined with scanning electron microscopy (SEM) and energy dispersive X-ray (EDX) investigations.

2. Experimental

2.1. Materials and chemicals

Polycrystalline powder of $SrNiP_2O_7$ (SNP) has been prepared by the conventional solid-state reaction technique [11]. Stoichiometric quantities of $SrCO_3$, $NiCO_3$ and

$(NH_4)H_2PO_4$ were well ground, mixed and progressively heated first to 473 K to expel NH_3 and H_2O and then to 1123 K for 10 hours.

The crystal structure of SNP was fully elucidated and presented in Fig. 1. Where Ni^{+2} is penta-coordinated by five oxygen atom belonging each a pyrophosphate P_2O_7 group. NiO_5 groups are not directly connected in the structure, their connection being made through O-P-O-P-O pyrophosphate's bridges.

The test solution used in the study is seawater solution (pH = 7.8) that collected from the red sea water (Egyptian coastal). The composition of the seawater is given in Table 1.

The SNP is added to the test solution at concentrations of for 20 to 180 mg/L. Powder of SNP is dissolved in of 1.0 M nitric acid and then added to test solution. The solution in the absence of SNP was taken as blank solution. The temperature of the mixture was controlled by an aqueous thermostat.

For mass loss experiments, the copper electrodes (99.999%) were mechanically cut into 2.2 cm × 1.2 cm × 0.2 cm dimensions. For electrochemical tests, the copper electrodes were embedded in epoxy resin with a geometrical surface area of 0.442 cm^2 exposed to the test solutions. Prior to all experiments, the copper electrode was abraded with emery paper of increasing fineness of up to 1200 grit. The copper electrode was then washed with distilled water, degreased with acetone and ethanol, washed using distilled water again, and finally dried.

2.2. Mass loss measurements

The mass loss was calculated by weighing the cleaned copper electrodes before and after immersion in seawater solution for 10 days at 298 K. The mass loss experiments were carried out in triplicate and the mean value of the mass loss is reported. The corrosion rate (C_R) in mg cm^{-2} h^{-1} has been calculated using the following equation:

$$C_R = \frac{W}{St} \quad (1)$$

where W is the mass loss (mg), S is the electrode surface area (cm^2) and t is the immersion time (h).

2.3. Electrochemical measurements

Polarization and electrochemical impedance spectroscopy (EIS) were carried out using ACM instruments Potentiostat/Galvanostat (Gill AC Serial no. 947).

All electrochemical experiments were carried out in the newly designed water-jacketed electrolytic cell as previously reported [17]. In this cell a copper metal, a platinum sheet and a saturated calomel electrode (SCE) were used as working, auxiliary and reference electrodes, respectively.

For polarization experiments the potential was in the potential range of ± 200 mV relative to the open circuit potential with a scan rate of 2.5 mV s^{-1}.

EIS measurements were carried out in frequency in the range 10 mHz –100 kHz with an amplitude of 10 mV peak-to-peak using ac signals at open circuit potential. Before EIS experiment, the copper electrode was immersed in test solutions for 1 h until it reaches a steady state condition.

Each electrochemical experiment has been repeated three times under the same conditions, and the mean values and standard deviations of the results are reported. In general, no significant variations in the repetitions for each concentration were observed.

2.4. The surface morphology investigations

The surface morphology of copper specimens after immersed in seawater solution for 10 days at 298 K with and without $SrNiP_2O_7$ were characterized by a digital

camera (KODAK EASYSHARE P850 zoom digital camera) and JEOL-JEM 1200 EX II scan electron microscope.

Energy dispersive X-ray spectroscopy (EDX) investigations were carried out in order to identify the elemental composition of the species formed on the metal surface. EDX examinations were carried out using a Traktor TN-2000 energy dispersive spectrometer

3. Results and discussion

3.1. Mass loss measurements

The value of inhibition efficiency (η_W %) and corrosion rate (C_R) obtained from mass loss method at different concentrations of SNP in seawater in recirculating system with solution flow rate of 0.8 m s^{-1} at 298 K are recorded in Table 2. The η_W % values were calculated from the following relation:

$$\eta_W\,\% = \frac{C_{R0} - C_R}{C_{R0}} \times 100 \qquad (2)$$

where C_{R0} and C_R are the corrosion rate without (blank) and with the inhibitor (SNP), respectively.

It is apparent that the corrosion rate of copper in seawater decreases obviously as SNP is added into seawater, and the inhibition efficiency increases with the increasing seawater concentration. The maximum inhibition efficiency form mass loss data (92.7%) is at 120 mg/L. No significant changes in the η_W % values at higher SNP concentration (> 120 mg/L). These results confirm that this inhibitor had good corrosion inhibition even at low concentrations. These results suggest that the SNP acts as fairly efficient inhibitor for copper corrosion in seawater.

3.2. Polarization measurements

3.2.1 Effect of SNP concentration

Fig. 2 shows typical polarization curves (Tafel plots) for copper in absence and presence of various concentrations of SNP in seawater in recirculating system with solution flow rate of 0.8 m s^{-1} at 298 K.

Electrochemical parameters, such as corrosion potential (E_{corr}) and corrosion current density (j_{corr}) are presented in Table 3. The corrosion current densities (j_{corr}) decrease greatly once SNP is added into the blank solution.

The presence of SNP remarkably shifts the E_{corr} towards cathodic potentials. Furthermore, the displacement in ΔE_{corr} ($E_{corr\ (Blank)} - E_{corr\ (in\ the\ presence\ of\ inhibitor)}$) is less than 85 mV. Therefore, the SNP can be defined as mixed type inhibitor with predominantly cathodic effectiveness [18].

The inhibitor efficiency of SNP (η_j %) was evaluated from polarization measurements using the following equation [19] :

$$\eta_j\% = \frac{j_{corr(0)} - j_{corr}}{j_{corr(0)}} \times 100 \qquad (3)$$

where $j_{corr(0)}$ and j_{corr} are the corrosion current densities in the absence and presence of SNP respectively.

The inhibition efficiencies obtained from the polarization data (Table 3) increase with the SNP concentration. Maximum inhibition performance (η_j % = 94.8) of SNP was achieved at 120 mg/L.

3.2.2. Effect of temperature

The effect of temperature on the inhibitor efficiency of SNP for copper in seawater containing 120 mg/L SNP, in the above mentioned conditions, was studied using polarization data at temperature ranging from 303 to 333 K.

The results are presented in Fig.3 and Table 4. It is clear that that the rate of copper corrosion (j_{corr}) in seawater in recirculating system containing SNP increases with

temperature while the inhibitor efficiency SNP decreases. Increasing the temperature leads to desorption of SNP form the copper metal surface. This causes a decrease in the inhibitor efficiency [20].

The Arrhenius equation gives the quantitative basis of the relationship between the activation energy and the corrosion rate [21]. From the Arrhenius equation, the activation energy can be expressed as [22]:

$$j_{\text{corr}} = A\exp(\frac{-E_a}{RT}) \quad (4)$$

where R is the molar gas constant, T is the absolute temperature and A is the frequency factor.

The Arrhenius plots in the absence (blank) and presence of 120 mg/L of SNP are presented in Fig. 4. The extracted values of E_a are 15.18 and 28.27 kJ mol^{-1} in absence and presence 120 mg/L of SNP, respectively. The higher E_a value in the presence of 120 mg/L of SNP in comparison to that obtained in blank solution can be correlated with physical adsorption phenomenon by SNP molecules on copper surface. This indicates that the more energy barrier for the corrosion reaction in the presence of SNP is obtained [23].

3.3. EIS measurements

Typical Nyquist plots obtained for copper in absence and presence of various concentrations of SNP in seawater in recirculating system with solution flow rate of 0.8 m s^{-1} at 298 K are shown in Fig. 5. It has been found that all the impedance spectra obtained show a single depressed capacitive loop which is related to charge transfer of the corrosion process [24-25]. The diameters of the capacitive loops increase with increasing SNP concentration. The roughness and in-homogeneities of the copper surface cause non perfect semicircle [26]. EIS data are commonly analyzed

by fitting it to an equivalent electrical circuit model. The equivalent circuit model used to fit EIS results is shown in Fig. 6. In this circuit R_s is the resistance of the solution, R_{ct} is the charge transfer resistance and CPE_{dl} is the constant phase element. Capacitors in EIS experiments often do not behave ideally. Instead, they act like a constant phase element (CPE_{dl}). Impedance parameters (R_{ct} and CPE_{dl}) in absence and presence of various concentrations of SNP were analyzed using Sequencer software and are shown in Fig.7. As shown in Fig.7, the addition of SNP increases the R_{ct} values and this effect seems to be enhanced upon the increasing of SNP concentration. On other hand, the CPE_{dl} values decrease with the increasing of SNP concentration. This behavior is perhaps due to the replacement of water molecules by the adsorption of SNP molecules at copper/seawater solution interface, which leads to a protective film adsorbing on the metal surface [27].

Since the reciprocal of the charge transfer resistance (R_{ct}^{-1}) corresponds to the corrosion rate of a metal in corrosive solutions, the inhibition efficiency (η_R %) of SNP can be calculated using the following equation [28] :

$$\eta_R\,\% = \frac{R_{ct} - R_{cto}}{R_{ct}} \times 100 \qquad (5)$$

where R_{ct} and R_{ct0} are the charge transfer resistances in the presence and absence of SNP, respectively.

Fig. 8 illustrates plot of η_R % versus SNP concentration. The data clearly show that, the inhibition efficiency increases with increasing SNP concentration reaching a maximum value (97.1%) at 120 mg/L concentration.

This data confirms the data obtained by mass loss and polarization measurements and provides further evidence of the ability SNP as a good corrosion inhibitor.

By comparing the results, it is observed that the inhibition efficiencies calculated from EIS measurements show the same trend as that obtained from polarization measurements and mass loss measurements.

3.4. Adsorption isotherm of SNP

The data obtained from adsorption isotherms are very important in the description the adsorption process of SNP on the copper surface. A wide variety of adsorption isotherms have been formulated to describe how adsorbed molecules interact with the adsorbent materials [29]. Freundlich isotherm is the earliest known relationship describing the non-ideal and reversible adsorption, not restricted to the formation of monolayer. We adopted it in this work to describe the adsorption process of SNP on the copper surface**.** This empirical model can be applied to multilayer adsorption on the heterogeneous surface [30]. According to this model, there is a relation between the surface coverage (θ) and inhibitor concentration (C_{inh}), as follows:

$$\theta = K_F (C_{\text{inh}})^{1/n} \qquad (6)$$

The linear form of Freundlich isotherm is represented by the equation:

$$\log(\theta) = \log K_{\text{F}} + \frac{1}{n} \log C_{\text{inh}} \qquad (7)$$

where K_F is the Freundlich constant indicative of the relative adsorption capacity of the adsorbent. The Freundlich slope ($1/n$), ranging between 0 and 1, is a measure of adsorption intensity or surface heterogeneity. In fact, a value close to zero means heterogeneous surface; whereas, a value below unity implies chemisorptions process and above is an indicative of cooperative adsorption [31]. The experimental data from mass loss, polarization and EIS measurements were used for presenting the linear Freundlich isotherm (Fig.9). The surface coverage degree θ can be calculated from

mass loss and polarization and EIS measurements using the relations (η_w %/100), (η_j %/100) and (η_R%/100), respectively.

The linear Freundlich isotherm parameters for adsorption SNP on the copper surface are listed in Table 5. The regression coefficient (r^2) is employed to analyze the fitting degree of isotherm with the experimental data, where its values vary from 0 to 1 [32]. The high correlation coefficients of 0.9837, 0.9786 and 0.9842 confirms that the adsorption of SNP on the copper surface consistent with the Freundlich isotherm. The value of $1/n$ located between 0 and 1 confirms the favorable conditions for adsorption.

The Freundlich constant K_F can be used to calculate the standard free energy of SNP adsorption (ΔG^0_{ads}) on the copper surface using the following equation [33]:

$$\Delta G^o_{ads} = -RT \ln(55.5K_F) \quad (8)$$

where R is the molar gas constant (J K^{-1} mol^{-1}), T is the absolute temperature (K) and 55.5 is the concentration of water in solution expressed in molar.

The ΔG^o_{ads} values calculated form mass loss, polarization and EIS data are -30.1, -30.7, -30.8 kJ mol^{-1}, respectively.

It is clear that ΔG^o_{ads} values have negative sign and less than -40 kJ mol^{-1}. This indicates that the adsorption of SNP on the copper surface will be favored and will release energy. Furthermore, the type of adsorption is regarded as physical adsorption [34].

3.5. Surface morphology observation

The formation of a complex layer by inhibitor adsorption on the metal surface was confirmed by surface morphology observation.

The macroscopical of copper specimens before and after immersed in seawater solution for 10 days at 298 K with and without SNP are shown in Fig. 10. Compared with the copper specimen before the immersion (Fig. 10a), the surface in the absence of SNP (Fig. 10b) is strongly corroded and the copper surface contains several pits and the yellow-brown corrosion product (anhydrous $CuCl_2^-$). However, in the presence of SNP (Fig. 10c), the specimen surface is well protected where the surface characterized by forming a red-orange film on the copper surface. This film is mainly due to SNP adsorption.

Further Surface morphology observation was carried out using SEM micrographs of copper specimens before and after immersed in seawater solution for 10 days at 298 K with and without SNP (Fig. 11). It is clearly observed that the copper surface morphology was strongly damaged by exposing to seawater without SNP (Fig.11a). While in the case of inhibited solution (seawater + 120 mg/L SNP) (Fig. 11c), the surface of copper specimen was smoother and less pits. This clearly proves that the corrosion process was suppressed via forming adsorbed layer of SNP on the copper surface.

The EDX spectra after the immersion in the blank solution (seawater) (Fig. 12a) show some peaks of copper and chloride. This indicates that the corrosion products on the copper surface are mainly CuCl and /or $CuCl_2^-$. On the other hand, the EDX spectra (Fig.12b) recorded for copper in the presences of 120 mg/L SNP show that the peak due to the chloride decreased dramatically. This suggests that there is much less corrosion product at the metal surface. Compared with the blank (without SNP), the EDX spectra (Fig.12b) show additional signals characteristic for the elements O, P, Ni, and Sr. It confirms that the SNP has directly adsorbed onto the copper surface to form a protective film.

3.6. The mechanism of corrosion inhibition by SNP

The corrosion mechanisms of copper in seawater can be described as follows [35-36]:

i) The cathodic reaction:

$O_2 + 2H_2O + 4e \rightarrow 4OH^-$ (9)

ii) The anodic reactions

$Cu \rightarrow Cu^+ + e$ (10)

$Cu^+ + Cl^- \rightarrow CuCl$ (11)

Because of the very weak adhesion and stability of The CuCl layer formed on copper surface, it reacts with chloride ions to form soluble cuprous chloride complex $CuCl_2^-$ (equation 12).

$CuCl + Cl^- \rightarrow CuCl_2^-$ (12)

Finally, chloride complex $CuCl_2^-$ moves from the copper surface to the bulk solution and formed Cu^{+2} and Cl^- ions (equation 13).

$CuCl_2^- \rightarrow Cu^{+2} + 2Cl^- + e$ (13)

The data obtained form mass loss, polarization and EIS measurements indicate that SNP is one of the effective corrosion inhibitor for copper metal in seawater. SNP acts through adsorption on copper surface blocking the active sites by displacing water molecules and forming a barrier film to decrease the corrosion rate [37-38]. The mechanism seems to be relatively well resolved when the inhibiting molecular reacts on a clean surface such as polyphosphate. The adsorption of inhibitors on the corroded metal is affected by several parameters like the type of metal, the charge of metal surface, electrolyte pH, temperature, ions present in electrolyte and molecular geometry, electronic structure and crystal structure of the inhibitors molecules [39-40].

Form the chemical structure of SNP molecule; we could propose that Sr^{2+} atoms in SNP can interact with $CuCl_2^-$ species which are formed in equation (12) through electrostatical force, and then prevent oxidation reaction (equation 13). In the same time, owing to lone-pair electrons of O atoms, SNP molecules may combine with Cu^{+2} ions to form the metal inhibitor complexes. These complexes might get adsorbed onto copper surface by van der Waals force to form a protective barrier that separate between the copper surface and the seawater solution.

4. Conclusion

SNP was synthesized as powder and tested as a new inorganic inhibitor for the corrosion of copper metal in recirculating cooling sea water. The inhibition performance obtained from mass loss data shows the same trend as noticed in electrochemical data. The highest inhibition efficiency obtained from mass loss, polarization and EIS measurements are 92.7, 94.8 and 97.1% respectively at 120 mg/L concentration. The Polarization curves suggest that SNP classified as a mixed-type inhibitor with predominantly cathodic effectiveness. The rise in temperature suppresses the adsorption of the SNP on the copper surface and accelerates the corrosion process. The best correlation between the experimental results and the isotherms was obtained using Freundlich isotherm. Surface morphology observation supported that SNP formed protective layer copper surface during the inhibition process.

References

[1] Z. Foroulis, Inhibition of corrosion in cooling water systems with mixtures of gluconate salts and silicate salts, US Patent 3711246 A, 1973.

[2] P. Verma, Cooling Water Treatment Hand Book. India: Albatross Fine LTD (Book Division), 2004.

[3] R. Harish, E. E. Subhramanyan, R. Madhavan, S. Vidyanand, Theoretical model for evaluation of variable frequency drive for cooling water pumps in sea water based once through condenser cooling water systems, Appl. Therm. Eng., 2010, 30, 2051-2057.

[4] P. J. Karditsas, S. M. Ali, D. Wan, Copper corrosion and activation in water cooling loops under fusion irradiation conditions, J. Nucl. Mater., 2000, 283, 1346-1350.

[5] A. Drach, I. Tsukrov, J. DeCew, J. Aufrecht, A. Grohbauer, U. Hofmann, Field studies of corrosion behavior of copper alloys in natural seawater, Corros. Sci., 2013, 76, 453-464.

[6] L. Núñez, E. Reguera, F. Corvo, E. González, C. Vazquez, Corrosion of copper in seawater and its aerosols in a tropical island, Corros. Sci., 2005, 47, 461-484.

[7] J. Sandberg, I. O. Wallinder, C. Leygraf, N. Le Bozec, Corrosion- induced copper runoff from naturally and pre-patinated copper in a marine environment, Corros. Sci., 2006, 48, 4316-4338.

[8] M. M. Antonijevic, M. B. Petrovic, Copper Corrosion Inhibitors. A review, Int. J. Electrochem. Sci., 2008, 1 – 28.

[9] A. Bahadur, Development and evaluation of a low chromate corrosion inhibitor for cooling water systems, Can. Metall. Quart., 1998, 37, 459-468.

[10] G. Bierwagen, R. Brown, D. Battocchi, S. Hayes, Active metal-based corrosion protective coating systems for aircraft requiring no-chromate pretreatment, Prog. Org. Coat. 2010, 68, 48-61.

[11] B. El-Bali, A. Boukhari, J. Aride, K. Maaß, D. Wald, R. Glaum, F. Abraham, Crystal structure and colour of $SrNiP_2O_7$ and $SrNi_3(P_2O_7)_2$, Solid State Sci., 2001, 3, 669–676.

[12] H. M. Nykyforchyn, Z. V. Slobodyan, D. M. Zaverbnyi, Effect of pyrophosphate-polyphosphate inhibitors on the processes of corrosion and salt deposition in aqueous systems, Mater. Sci., 1997, 33, 346-357.

[13] J. E. Lee, H. D. Lee, G. E. Kim, The Effect of Corrosion Inhibitor on Corrosion Control of Copper Pipe and Green Water Problem, Environ. Eng. Res., 2012, 17, 17-25.

[14] S. Chen, L.-h. Jiang, J.-x. Xu, Corrosion Inhibition Property of Sodium Pyrophosphate in Simulated Concrete Pore Solution, Corrosion & Protection, 2012, 33, 5-7.

[15] N. Etteyeb, L. Dhouibi, M. Sanchez, C. Alonso, C. Andrade, E. Triki, Electrochemical study of corrosion inhibition of steel reinforcement in alkaline solutions containing phosphates based components, J. Mater. Sci., 2007, 42, 4721-4730.

[16] A. Majjane, D. Rair, A. Chahine, M. Et-tabirou, M. Ebn Touhami, R. Touir, Preparation and characterization of a new glass system inhibitor for mild steel corrosion in hydrochloric solution, Corros. Sci., 2012, 60, 98-103.

[17] M. A. Deyab, The influence of different variables on the electrochemical behavior of mild steel in circulating cooling water containing aggressive anionic species, J. Solid State Electrochem., 2009, 13,1737–1742.

[18] A. O. Yuce, B. D. Mert, G. Kardas, B. Yazıcı, Electrochemical and quantum chemical studies of 2-amino-4-methyl-thiazole as corrosion inhibitor for mild steel in HCl solution, Corros. Sci., 2014, 83, 310–316.

[19] M. A. Deyab, S. S. Abd El-Rehim, Effect of succinic acid on carbon steel corrosion in produced water of crude oil, J. Taiwan Inst. Chem. E., 2014, 45, 1065–1072.

[20] M. A. Deyab. Egyptian licorice extract as a green corrosion inhibitor for copper in hydrochloric acid solution, J. Ind. Eng. Chem., 2015, 22, 384–389

[21] K. J. Laidler, Chemical Kinetics, Third Edition: Harper & Row, 1987.

[22] M. A. Deyab, S. T. Keera, Effect of nano-TiO_2 particles size on the corrosion resistance of alkyd coating, Mater. Chem. Phys., 2014, 146, 406-411.

[23] Q. B. Zhang, Y. X. Hua, Corrosion inhibition of mild steel by alkylimidazolium ionic liquids in hydrochloric acid, Electrochim. Acta, 2009, 54, 1881–1887.

[24] M. A. Deyab, Adsorption and inhibition effect of Ascorbyl palmitate on corrosion of carbon steel in ethanol blended gasoline containing water as a contaminant, Corros. Sci., 2014, 80, 359–365.

[25] M. A. Deyab, S. S. Abd El-Rehim, Influence of Polyethylene Glycols on the Corrosion Inhibition of Carbon Steel in Butyric Acid Solution: Weight Loss, EIS and Theoretical Studies, Int. J. Electrochem. Sci., 2013, 8, 12613 – 12627.

[26] M. A. Deyab, Corrosion protection of aluminum bipolar plates with polyaniline coating containing carbon nanotubes in acidic medium inside the polymer electrolyte membrane fuel cell, J. Power Sources, 2014, 268, 50-55.

[27] M. A. Deyab, Hydrogen generation during the corrosion of carbon steel in crotonic acid and using some organic surfactants to control hydrogen evolution, Int. J. Hydrogen Energy, 2013, 38, 13511-13519.

[28] S. T. Keera, M. A. Deyab, Effect of some organic surfactants on the electrochemical behavior of carbon steel in formation water, Colloids Surf. A Physicochem. Eng. Asp., 2005, 266,129–140.

[29] A. Malek, S. Farooq, Comparison of isotherm models for hydrocarbon adsorption on activated carbon, AIChE J., 1996, 42, 3191–3201.

[30] H. M. F. Freundlich, Over the adsorption in solution, J. Phys. Chem., 1906, 57, 385-471.

[31] M. R. Gandhi, N. Viswanathan, S. Meenakshi, Preparation and application of alumina/chitosan biocomposite, Int. J. Biol. Macromol., 2010, 47,146–154.

[32] D. Karadag, Y. Koc, M. Turan, M. Ozturk, Acomparative study of linear and nonlinear regression analysis for ammonium exchange by clinoptilolite zeolite, J. Hazard. Mater., 2007, 144, 432–437.

[33] Z. A. AL-Othman. Inamuddin, M. Naushad, Adsorption thermodynamics of trichloroacetic acid herbicide on polypyrrole Th(IV) phosphate composite cation-exchanger, Chem. Eng. J., 2011, 169, 38-42.

[34] M. A. Deyab, Hydrogen evolution inhibition by L-serine at the negative electrode of a lead–acid battery, RSC Adv., 2015, 5, 41365–41371.

[35] E. M. Sherif, R. M. Erasmus, J. D. Comins, Corrosion of copper in aerated synthetic sea water solutions and its inhibition by 3-amino-1,2,4-triazole, J. Colloid Interface Sci., 2007, 309, 470–477.

[36] H. Tian, W. Li, B. Hou, Novel application of a hormone biosynthetic inhibitor for the corrosion resistance enhancement of copper in synthetic seawater, Corros. Sci., 2011, 53, 3435–3445.

[37] M. A. Deyab, Effect of halides ions on H_2 production during aluminum corrosion in formic acid and using some inorganic inhibitors to control hydrogen evolution, J. Power Sources, 2013, 242, 86-90.

[38] E. Samiento-Bustos, J. G. G. Rodriguez, J. Uruchurtu, G. Dominguez-Patiño, V. M. Salinas-Bravo, Effect of inorganic inhibitors on the corrosion behavior of 1018 carbon steel in the LiBr + ethylene glycol + H_2O mixture, Corros. Sci., 2008, 50, 2296-2303.

[39] S. Zhang, Z. Tao, S. Liao, F. Wu, Substitutional adsorption isotherms and corrosion inhibitive properties of some oxadiazol-triazole derivative in acidic solution, Corros. Sci., 2010, 52, 3126–3132.

[40] Sh. Pournazari, M. H. Moayed, M. Rahimizadeh, situ inhibitor synthesis from admixture of benzaldehyde and benzene-1,2-diamine along with $FeCl_3$ catalyst as a new corrosion inhibitor for mild steel in 0.5 M sulphuric acid, Corros. Sci., 2013, 71: 20–31.

List of Figures

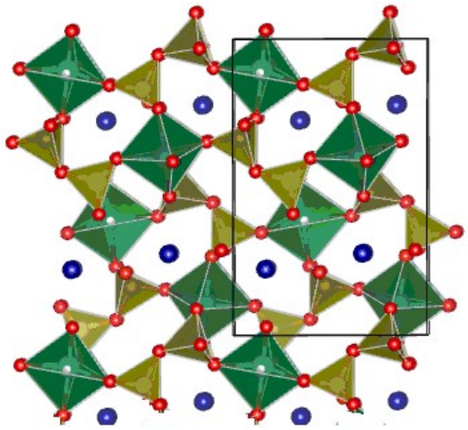

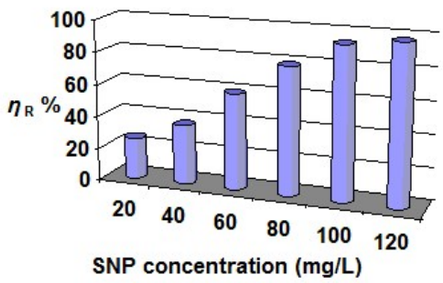

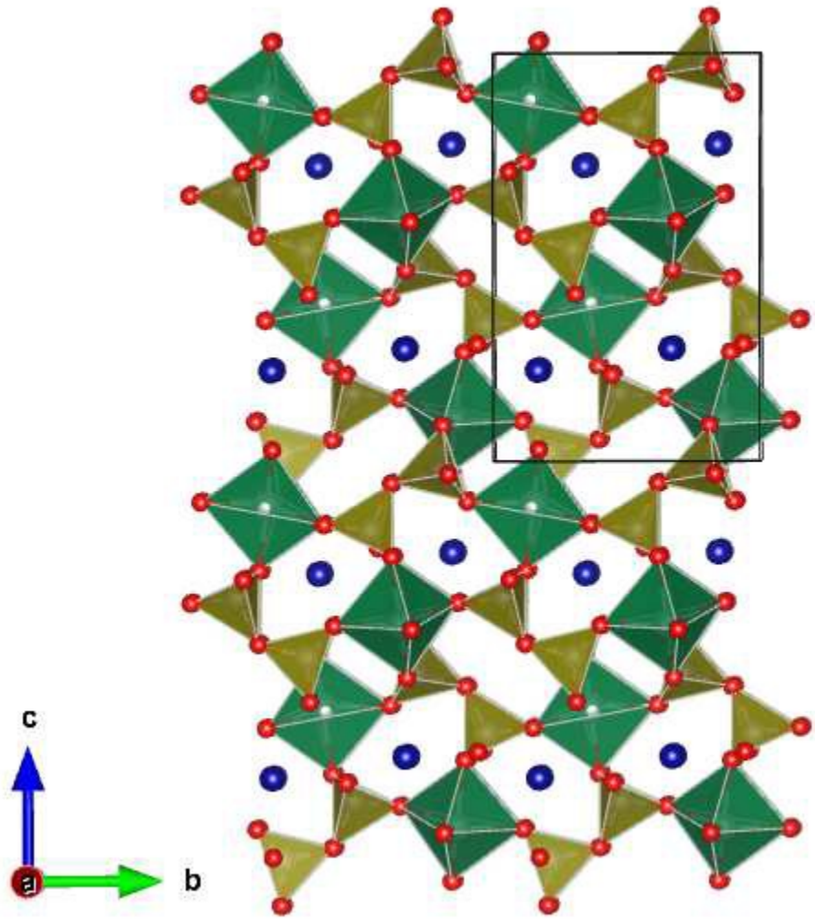

Fig.1

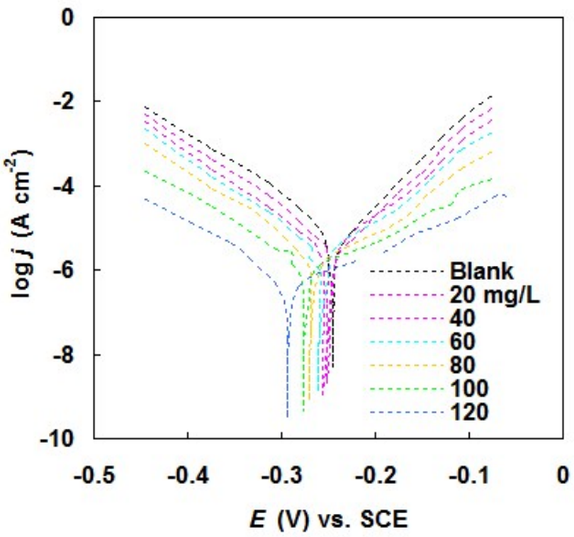

Fig.2

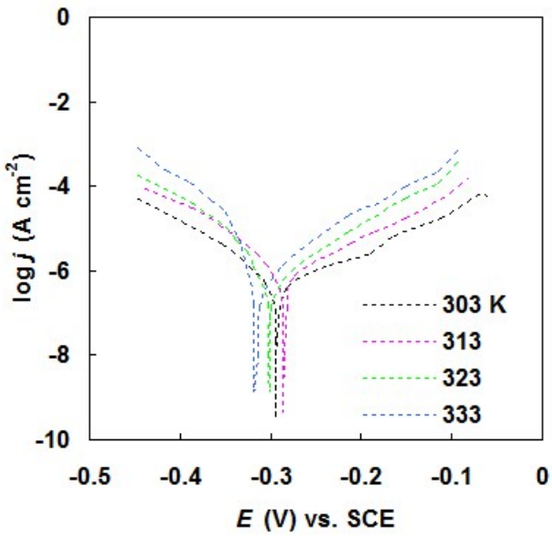

Fig.3

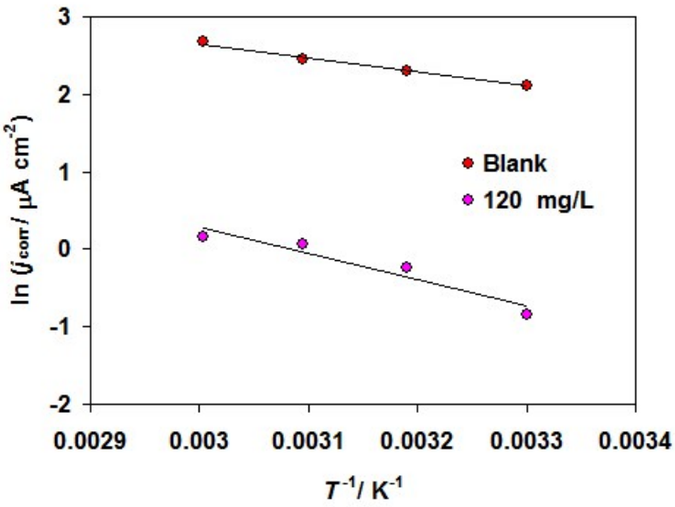

fig.4

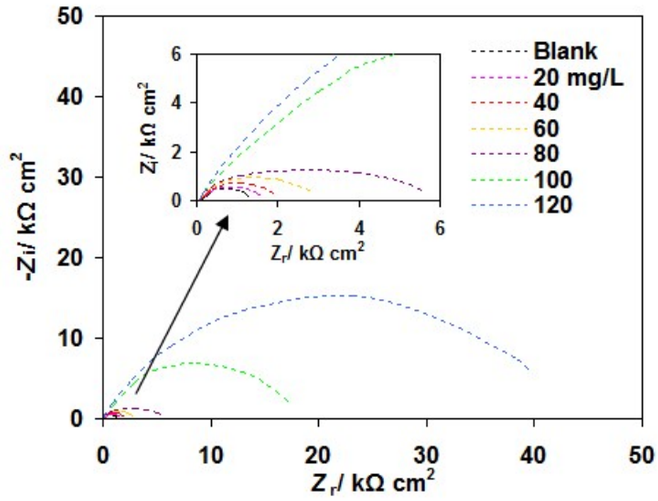

fig.5

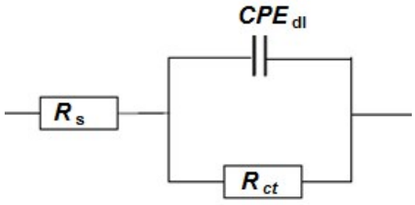

fig.6

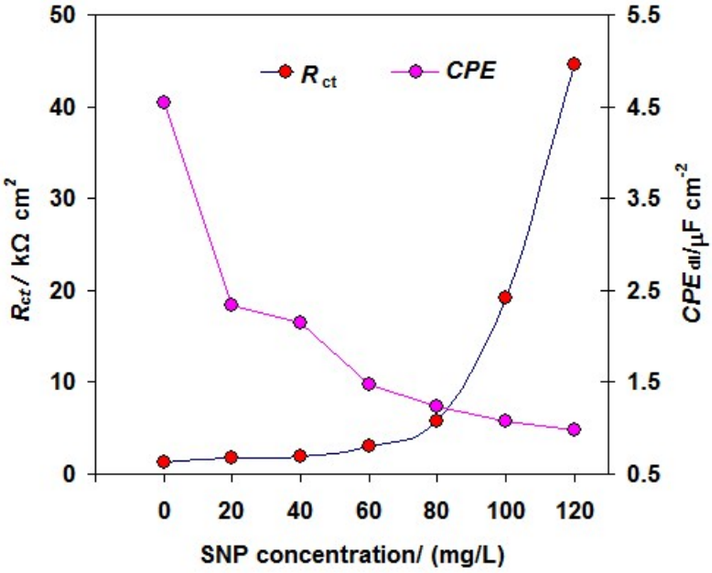

fig.7

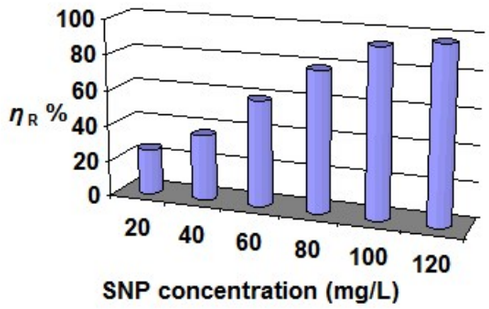

fig.8

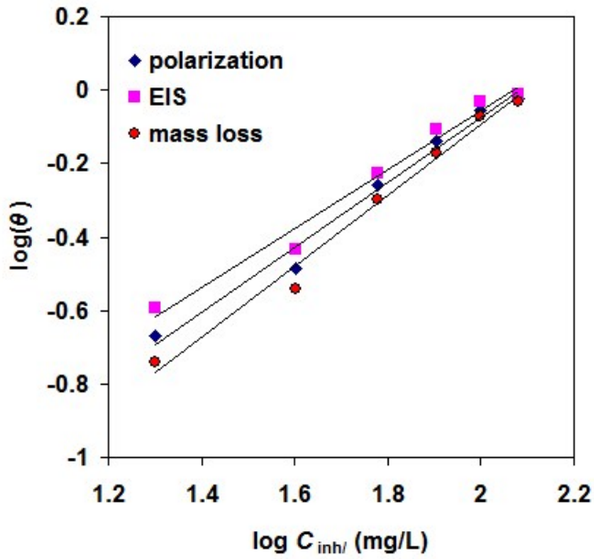

fig.9

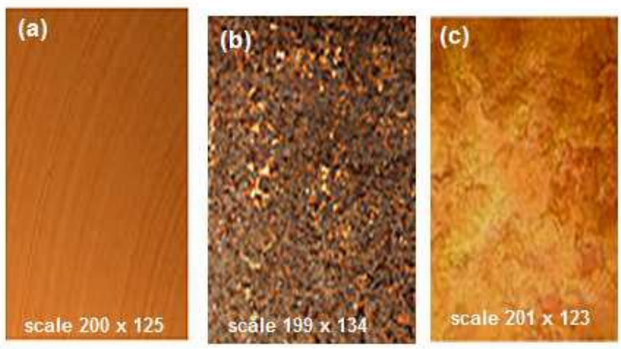

Fig 10

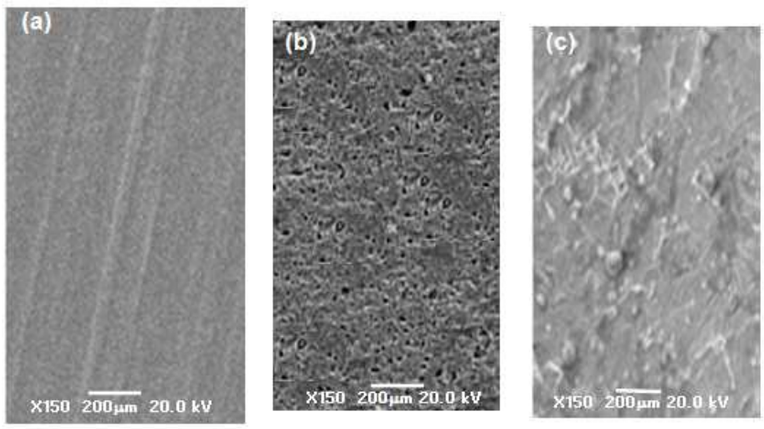

Fig.11

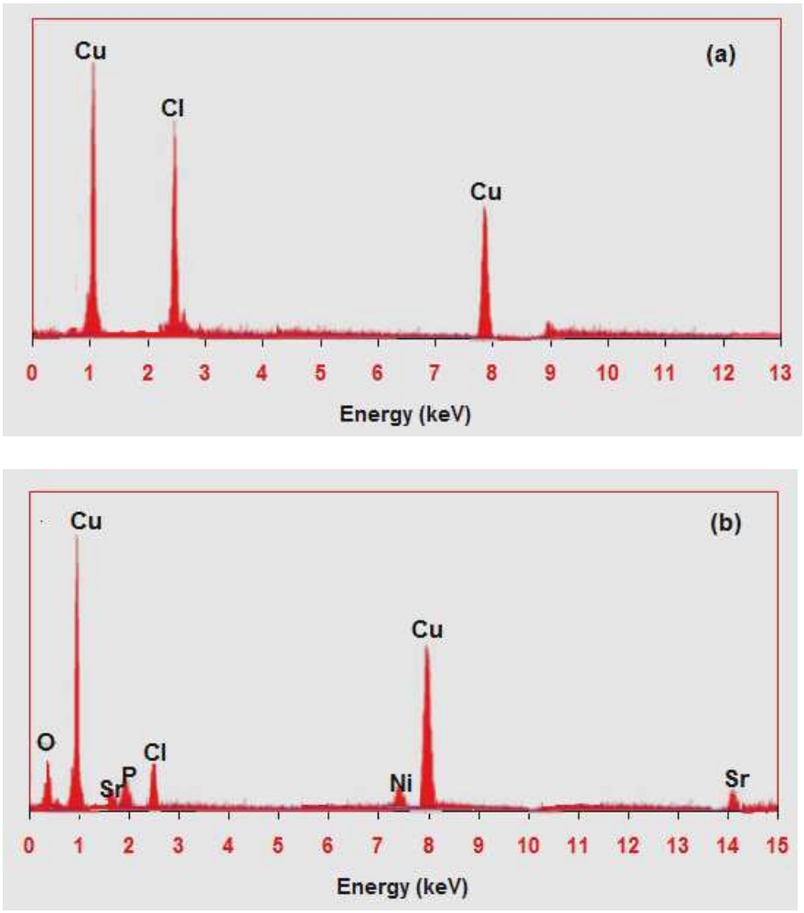

Fig.12